

## Porous titanium implants fabricated by metal injection molding

CHEN Liang-jian(陈良建)<sup>1,2</sup>, LI Ting(李挺)<sup>1</sup>, LI Yi-min(李益民)<sup>1</sup>,  
HE Hao(何浩)<sup>1</sup>, HU You-hua(胡幼华)<sup>1</sup>

1. State Key Laboratory of Powder Metallurgy, Central South University, Changsha 410083, China;
2. Department of Stomatology, Third Xiangya Hospital, Central South University, Changsha 410013, China

Received 16 May 2009; accepted 20 July 2009

**Abstract:** Sodium chloride (NaCl) was added as a space holder in synthesis of porous titanium by using metal injection molding(MIM) method. The microstructure and mechanical properties of porous titanium were analyzed by mercury porosimeter, scanning electron microscope(SEM) and compression tester. The results show that the content of NaCl influences the porosity of porous titanium significantly. Porous titanium powders with porosity in the range of 42.4%–71.6% and pore size up to 300  $\mu\text{m}$  were fabricated. The mechanical test shows that with increasing NaCl content, the compressive strength decreases from 316.6 to 17.5 MPa and the elastic modulus decreases from 3.03 to 0.28 GPa.

**Key words:** porous titanium; metal injection molding; porosity; compressive strength; elastic modulus

### 1 Introduction

Titanium(Ti) and its alloys are widely used for manufacturing orthopedic and dental devices under load bearing applications[1]. However, their long term clinical performances may be compromised by the different mechanical properties exhibited by titanium compared with bone, creating a stress shielding effect at the bone/implant interface[2–3]. Porous titanium presents diminished mechanical properties compared with the solid material, and porous titanium implant helps to reduce the stiffness mismatch between implant and bone tissue, thus reducing ‘stress shielding’ and achieving stable long-term fixation[4]. A porous implant material with adequate pore structure and appropriate mechanical properties has been sought as the ideal bone substitute. Open-cellular pores are necessary for bone ingrowth, and extensive body fluid transport through the porous scaffold matrix is possible, which can trigger bone growth if substantial pore interconnectivity is established[5–7]. Although increased porosity and pore size are obviously preferential for new bone growth in Ti implant[8–9], it should be kept in mind that another consequence of the porosity and pore size increase is the

reduction of the implant mechanical properties. Thus depending on the intended application, a balance between mechanical properties and biological performance should be found.

So, there is a demand for fabrication methods for bulk porous Ti of which the porosity, pore size and distribution, and mechanical properties can be controlled for biomedical applications[6]. A number of approaches to fabricate three-dimensionally porous titanium have been reported, including partial sintering of powders[10] or wires[11], and sintering of powders around a temporary space-holding phase[9,12]. Those methods could produce porous materials with high porosity and well interconnected structure, but porosity and pore size of materials are difficult to be controlled. So, porous materials need post-machining processes that could be detrimental to the integrity of the pore structure. Metal injection molding(MIM) could be an attractive process for overcoming this problem. It combines the technique of polymer injection molding with the advantages of PM. The possibility of near-net-shape production combined with a high potential for automation makes the MIM process suitable for the industrial production of porous Ti. The MIM process starts with the mixing of metal powder with one or more polymers to produce a feed-

stock, followed by molding of the homogenized feedstock into shape parts, removal of polymer and final sintering.

The aim of this work is to develop processes controlling the porosity and the pore structure for ensuring the desired homogeneity of the product. MIM was used to produce porous titanium. The effect of the content of space holder on the pore structure, i.e., porosity and pore size, was investigated. The influence of pore structure on compressive strength and elastic modulus was addressed and discussed.

## 2 Experimental

### 2.1 Materials

Hydrogenation-dehydrogenation titanium (HDH Ti) powder with a particle size  $< 77 \mu\text{m}$ , and sodium chloride (NaCl) powder with a particle size  $< 290 \mu\text{m}$  were used in this study. Morphologies of the powders are both irregular in shape, as shown in Fig.1. In order to evaluate the effect of different content of NaCl on porosity and pore size, five different feedstocks with different volume fractions of NaCl, 30%, 40%, 50%, 60% and 70% were prepared. A multi-component binder system was selected for this work. The binder consisted of a mixture of high density polyethylene (HDPE), paraffin wax (PW), polyethylene glycol (PEG) and stearic acid (SA). Mixing of binders and powders was conducted

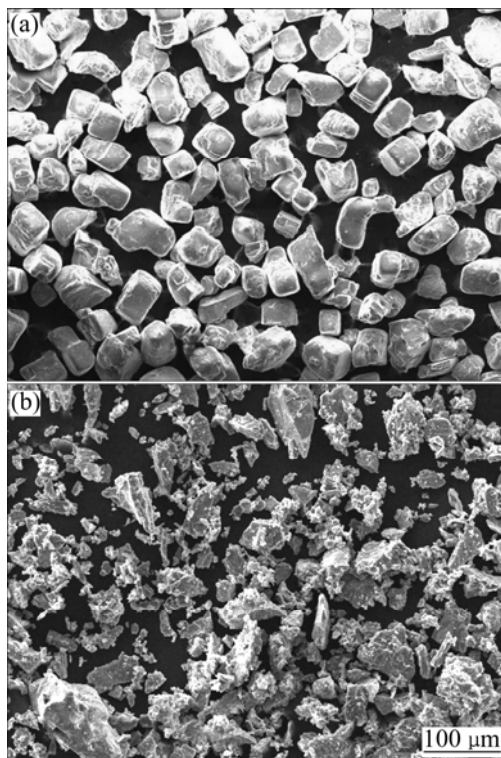


**Fig.1** Morphologies of initial powders: (a) NaCl powders; (b) Titanium powders

in a XSM1/20-80 rubber mixer with a pair of roller rotor blades at  $150 \text{ }^\circ\text{C}$  for 1 h. All the feedstocks were extruded twice to get homogeneous mixtures. After compounding, feedstocks were properly granulated.

### 2.2 Injection molding

Injection step was carried out in an injection molding machine (BOY50T2). Cylindrical samples were produced ( $d 12 \text{ mm} \times 8 \text{ mm}$ ). The injection molding parameters were optimized. Mold temperature was  $30 \text{ }^\circ\text{C}$ , injection temperature was  $155 \text{ }^\circ\text{C}$ , and injection pressure was 100 MPa.

### 2.3 Debinding and sintering

The organic part of compact was removed through solvent and thermal debinding. The space holder of compact was removed by water dissolving. Firstly, the solvent debinding was performed by immersion of compacts in methylene dichloride at  $37 \text{ }^\circ\text{C}$  for 2.5 h. Then, the space holder was removed in a water bath. Finally, thermal debinding was performed in argon atmosphere at  $720 \text{ }^\circ\text{C}$  in a tubular furnace. Binders and space holder should be removed clearly, which could be determined by mass loss measurement, avoiding pollution of sintering furnace. The compacts were sintered at  $150 \text{ }^\circ\text{C}$  for 2 h under a vacuum of  $1.33 \times 10^{-3} \text{ Pa}$ . Two heating rates were used: a slower heating rate  $4 \text{ K/min}$  to  $525 \text{ }^\circ\text{C}$  followed by a faster heating rate of  $10 \text{ K/min}$  to the final sintering temperature.

### 2.4 Testing methods

The density, open porosity, and general porosity were determined by Archimede's method with the theoretical density of  $4.5 \text{ g/cm}^3$  for titanium. Pore size and the distribution of the inter-pore connections were measured from the penetration of Hg vapor in an Autopore II 9220 evacuated porosimeter. The microstructures of the samples were observed using a JSM-6360 LV scanning electron microscope (SEM). Compression tests were carried out on the specimens with a size of  $d 12 \text{ mm} \times 8 \text{ mm}$  at room temperature according to ASTM 451 standard. Five samples of each material were tested under a compression load in a CMT-7205 screw driven universal testing machine at a strain rate of  $10^{-3} \text{ s}^{-1}$ . The tests were performed at  $37 \text{ }^\circ\text{C}$ .

## 3 Results and discussion

### 3.1 Dimensional shrinkage

For investigating the shrinkage quality, sample dimensions before and after sintering were measured.

Table 1 shows the amount of shrinkage in two dimensions. As can be seen that shrinkage is almost the same in two dimensions, indicating that the feedstock homogeneity is relatively good. Samples with 70% NaCl content were not presented in Table 1, for the samples collapsed and deformed during debinding.

### 3.2 Porosity and pore size distribution

The general porosity and open-pore ratio of the sintered porous alloys prepared from different feedstocks are also shown in Table 1. The open-pore ratio is defined as the ratio of the open porosity to the general porosity. As can be seen, the general porosity and open-pore ratio tend to increase with increasing addition amount of NaCl as space holder.

Fig.2 shows the results of mercury porosimeter analysis. The graph illustrates the diameters of the inter-pore connections. The vertical axis represents the number of inter-pore connections at each diameter. Therefore, the area under the curve means the total number of the connections. In samples 1 and 2, more than 90% of the inter-pore connections are smaller than 50  $\mu\text{m}$  in diameter. However, 45% of the inter-pore connections are larger than 50  $\mu\text{m}$  in sample 3 and 70% in sample 4. It is observed that the inter-pore connection size of sample depends greatly on the content of NaCl. With increasing NaCl content, vacancies caused by NaCl removing increase, and these vacancies are unable to be compensated by sintering, resulting in an increase in the number of macro-pore. And the micropores are mainly

**Table 1** Physical properties of MIM sintered samples

Sample No.	NaCl content/%	Dimensional shrinkage/%		General porosity/%	Open pore ratio/%
		Axial	Radial		
1	30	11.7	11.6	42.4±2.1	97.9
2	40	12.0	11.8	52.1±2.2	98.7
3	50	12.9	12.3	62.0±1.8	99.6
4	60	13.1	12.8	71.6±1.2	99.6

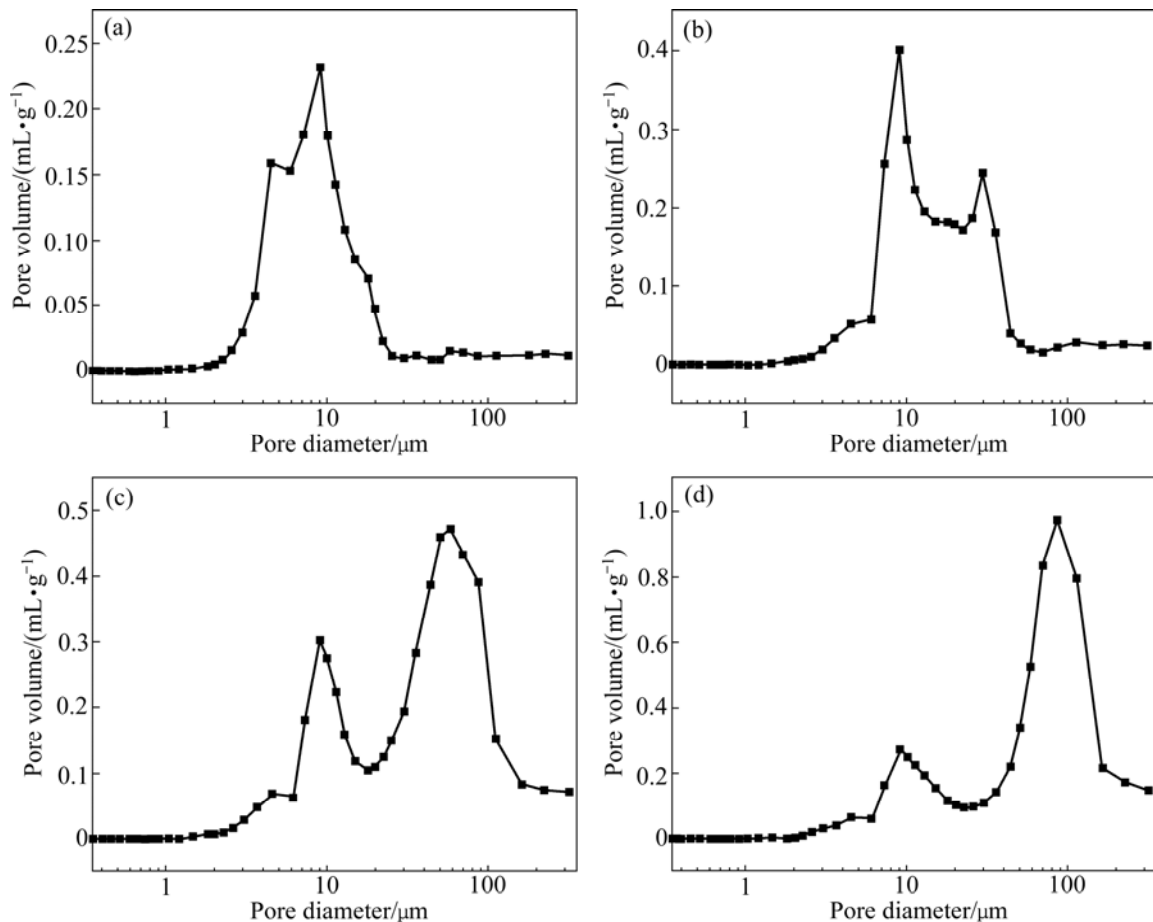


**Fig.2** Pore size distributions for porous titanium: (a) Sample 1; (b) Sample 2; (c) Sample 3; (d) Sample 4

caused by binders removal and the insufficient sintering of titanium powder. The results indicate that adding appropriate amount of NaCl in feedstocks can effectively control the pore size and porosity of final products.

### 3.3 Mechanical properties

Fig.3 shows the nominal stress—nominal strain curves of porous titanium with different addition of NaCl. As can be seen, the addition of NaCl has complex influence on the deformation behavior of porous titanium. These curves from different feedstocks show the same trend, i.e. a linear elastic deformation stage at the beginning of deformation, a long plateau stage with a nearly constant flow stress to large strain, and a densification stage where the flow stress rapidly increases. Open-cell porous materials are deformed primarily by cell-wall bending. Elastic modulus is the initial slope of the stress—strain curve. The long horizontal plateau in the stress—strain curve means that the material is strained at constant stress and that the strain produced is no longer recoverable. This plastic failure mechanism is of great interest since these materials can be used as energy absorbers, which can effectively buffer external stress and play an impact-resistance effect. This is important for bear-loading materials in biomedical application.

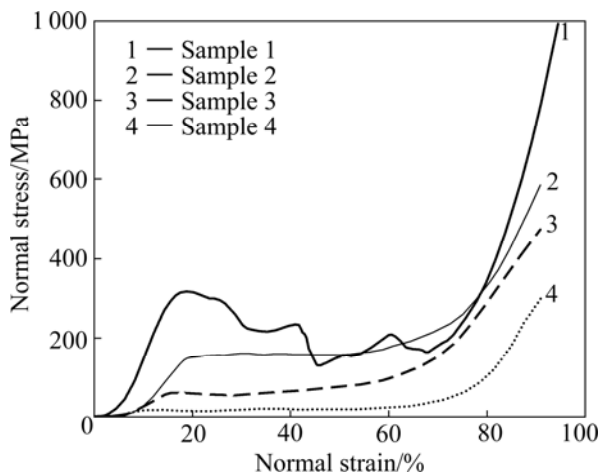


**Fig.3** Nominal stress—nominal strain curves of porous titanium samples fabricated by MIM with different NaCl content in feedstocks

The results of the mechanical properties are shown in Table 2. Special notice should be put on the elastic modulus because it plays a very important role in the design of biomaterials for bone substitution. If a bone replacement material is too stiff, it can stress-shield the surrounding living tissue. This means that the implant takes most of the load and the surrounding tissues sustain

loads well below their physiological level. There is clinical evidence that stress shielding is associated to resorption of the bone tissue adjacent to the implant, which leads to implant loosening and eventually to the subsequent implant failure. In this study, it can be observed that the values for four kinds of porous titanium samples are very similar to those of cancellous bone[13], especially those of the samples 3 and 4. The elastic modulus of the MIM processed porous Ti structures is in the range 0.28–3.03 GPa, which is comparable to natural bone. The low modulus of the porous titanium would prevent stress shielding and the bone ingrowth from the surrounding tissue would produce a good matching with the mechanical properties of the bone that the system is intended to be replaced[14]. The compressive strength of porous titanium depends on its porosity, and the strength increases from 17.5 to 316.6 MPa as the sample porosity decreases from 71.6% to 42.4%. The strength of the porous titanium with the highest porosity of 71.6% is approximately 17.5 MPa, which is presumably strong enough to resist handling during implantation and in vivo loading.

**Table 2** Mechanical properties of MIM porous titanium

Materials	General porosity/%	Compressive strength/MPa	Elastic modulus/GPa
Sample 1	42.4±2.1	316.6±11.4	3.03±2.10
Sample 2	52.1±2.2	157.1±15.7	1.50±1.80
Sample 3	62.0±1.8	63.2±12.8	0.95±0.60
Sample 4	71.6±1.2	17.5±3.8	0.28±0.20
Cancellous bone[14]	—	25.0±8.1	1.08±0.86

### 3.4 Microstructure characteristics

Porosity and pore size of porous implants both play a critical role in bone ingrowth. Some studies have reported that a pore size of 100–150  $\mu\text{m}$  is generally considered acceptable for cell size migration and transport, and higher porosity and larger pore size result in greater bone ingrowth[8,15–16]. In vivo, an interconnection size of over 20  $\mu\text{m}$  permits cell penetration and chondroid tissue formation inside macropores, and an interconnection size of over 50  $\mu\text{m}$  can assure mineralized bone formation[7]. In this study, the microstructures of four kinds of porous titanium samples are shown in Fig.4. It can be seen that there are two types of pores in the samples. One is a kind of interpenetrating macro-pores with the size in a range of 50–300  $\mu\text{m}$ , which is formed by spacer-holder removal. Macropores in sample 1 and 2 are mostly isolated (Figs.4(a) and (b)), those in sample 3 are partly interconnected (Fig.4(c)), and those in sample 4 are well

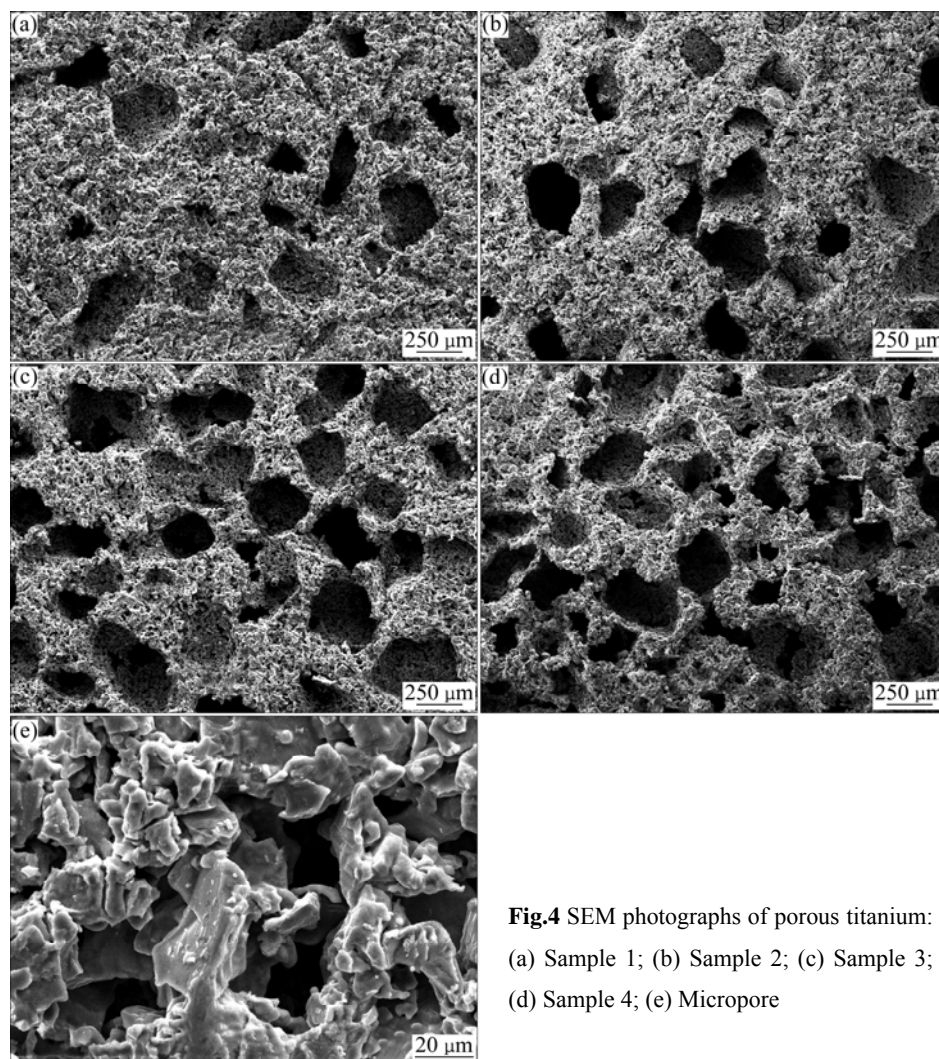


**Fig.4** SEM photographs of porous titanium:  
(a) Sample 1; (b) Sample 2; (c) Sample 3;  
(d) Sample 4; (e) Micropore

interconnected (Fig.4(d)). Simultaneously, other kinds of pores, much finer with a size of several micrometers, can be observed in Fig.4(e). The cell walls of the porous titanium are rough and honeycomb-like. The interconnected pore structure and rough wall-surface of macro-pores are appropriate for the in-growth of the new-bone tissues and the transport of the body fluids [17]. Samples 3 and 4 exhibit an open and interconnected porous structure. The result of mercury porosimeter analysis reveals that most of the inter-pore connections range from 50 to 300  $\mu\text{m}$ , and the elastic modulus and compressive strength for both titanium foams are very similar to those of cancellous bone. These results suggest that the samples 3 and 4 with adequate pore structure and appropriate mechanical properties would be used as the ideal bone substitute.

#### 4 Conclusions

1) Porous titanium with different porosities can be

fabricated by MIM with NaCl powder as space holder, and the porosity can be controlled by NaCl content adjustment.

2) In porous titanium with porosity of 62.0% and 71.6%, respectively, the macropores are well interconnected, and the mechanical properties are similar to those of cancellous bone.

3) MIM is a promising method to produce porous titanium for biomedical application.

#### References

- [1] HAYASHI K, UENOYAMA K, MATSUGUCHI N, SUGIOKA Y. Quantitative analysis of in vivo tissue responses to titanium-oxide and hydroxyapatite-coated titanium alloy [J]. *Journal of Biomedical Materials Research*, 1991, 25(4): 515–523.
- [2] YAO J, GLANT T T, LARK M W, MIKECZ K, JACOBS J J, HUTCHINSON N I, HOERRNER L A, KUETTNER K E, GALANTE J O. The potential role of fibroblasts in periprosthetic osteolysis: Fibroblast response to Ti particles [J]. *Journal of Bone and Mineral Research*, 1995, 10(9): 1417–1427.
- [3] BARRERE F, van der VALK C M, MEIJER G, DALMEIJER, R A J,

- de GROOT K, LAYROLLE P. Osteointegration of biomimetic apatite coating applied onto dense and porous metal implants in femurs of goats [J]. *Journal of Biomedical Materials Research*, 2003, 67B(1): 655–665.
- [4] KROGER H, VENESMAA P, JURVELIN J, MIETTINEN H, SUOMALAINEN O, ALHAVA E. Bone density at the proximal femur after total hip arthroplasty [J]. *Clinical Orthopaedics and Related Research*, 1998, 352: 66–74.
- [5] HEAD W C, BAUK D J, EMERSON R H. Titanium as the material of choice for cementless femoral components in total hip arthroplasty [J]. *Clinical Orthopaedics and Related Research*, 1995, 311: 85–90.
- [6] RYAN G, PANDIT A, APATSIDIS D P. Fabrication methods of porous metals for use in orthopaedic applications [J]. *Biomaterials*, 2006, 27(13): 2651–2670.
- [7] LU J X, FLAUTRE B, ANSELME K, HARDOUIN P, GALLUR A, DESCAMPS M, THIERRY B. Role of interconnections in porous bioceramics on bone recolonization in vitro and in vivo [J]. *Journal of Materials Science: Materials in Medicine*, 1999, 10(2): 111–120.
- [8] KARAGEORGIU V, KAPLAN D. Porosity of 3D biomaterial scaffolds and osteogenesis [J]. *Biomaterials*, 2005, 26(27): 5474–5491.
- [9] BRAM M, STILLER C, BUCHKREMER H P, STOVER D, BAUR H. High porosity titanium, stainless steel, and superalloy parts [J]. *Advanced Engineering Materials*, 2000, 2(4): 196–199.
- [10] OH I H, SEGAWA H, NOMURA N, HANADA S. Microstructures and mechanical properties of porosity-graded pure titanium compacts [J]. *Materials Transactions*, 2003, 44(4): 657–660.
- [11] MURRAY G A W, SEMPLE J C. Transfer of tensile loads from a prosthesis to bone using porous titanium [J]. *Journal of Bone & Joint Surgery, British Volume*, 1981, 63-B(1): 138–141.
- [12] WEN C, MABUCHI M, YAMADA Y, SHIMOJIMA K, CHINO Y, ASAHINA T. Processing of biocompatible porous Ti and Mg [J]. *Scripta Materialia*, 2001, 45(10): 1147–1153.
- [13] ELICES M. *Structural biological materials: Design and structure–property relationships* [M]. New York: Pergamon Press, 2000: 31–72.
- [14] SHIMKO D A, SHIMKO V F, SANDER E A, DICKSON K F, NAUMAN E A. Effect of porosity on the fluid flow characteristics and mechanical properties of tantalum scaffolds [J]. *Journal of Biomedical Materials Research Part B: Applied Biomaterials*, 2005, 73(2): 315–324.
- [15] UCHIDA A, NADE S, MCCARTNEY E, CHING W. Bone ingrowth into three different porous ceramics implanted into the tibia of rats and rabbits [J]. *Journal of Orthopaedic Research*, 1985, 3(1): 65–77.
- [16] DACULSI G, PASSUTI N. Effect of the porosity for osseous substitution of calcium phosphate ceramics [J]. *Biomaterials*, 1990, 11: 86–87.
- [17] NIHOJANNEN D L E, DACULSI G, SAFFARZADEH A, GAUTHIER O, DELPLACE S, PILET P, LAYROLLE P. Ectopic bone formation by microporous calcium phosphate ceramic particles in sheep muscles [J]. *Bone*, 2005, 36(6): 1086–1093.

(Edited by YANG Hua)